Hyperfine Structure in $O^{17}H$ and the OH Dipole Moment*†

GERALD EHRENSTEIN‡
Columbia University, New York, New York
(Received 11 December 1962)

A microwave spectrometer for the study of free radicals or other reactive species is described; it can be used with either Stark or Zeeman modulation. This spectrometer was used to determine the hyperfine structure of $O^{17}H$. Four main lines of the $^2\pi_{3/2}$, $J=7/2$ Λ-doubling transition were definitely observed, and there is evidence that one satellite line was also detected. Quantum number assignments were made for the four main lines, which are divided into two doublets. In the course of establishing the uniqueness of these assignments, the Λ-doubling frequency for the $^2\pi_{3/2}$, $J=7/2$ state of $O^{18}H$ was experimentally determined. The separation between doublets in the $O^{17}H$ spectrum was used to determine the hyperfine constant d associated with the O^{17} nucleus. The constant d was also computed theoretically from a simple molecular model of OH in which a single unpaired $p\pi$ electron about the O^{17} nucleus is assumed. The experimental value is about 8% greater in magnitude than the theoretical value, and this difference is discussed. The same spectrometer was used for the determination of the electric dipole moment of OH by measuring the Stark shift of the $^2\pi_{3/2}$, $J=7/2, M=4$ Λ-doubling line of $O^{16}H$ at a known electric field. The OH dipole moment was found to be 1.60 ± 0.12 D.

I. INTRODUCTION

MICROWAVE spectroscopy has been used previously to determine the hyperfine coupling constants of $O^{16}H$.[1,2] These constants give information concerning the unpaired electron distribution about the proton. A simple interpretation of this information cannot be made, however, because the oxygen nucleus is well within the $2p$ electron orbit of the proton, and a $2p$ atomic orbital would hence be a very poor approximation.[1] Experimental results on $O^{17}H$, on the other hand, give information concerning the unpaired electron distribution about the oxygen nucleus. A $2p$ atomic orbital about the oxygen nucleus may be a reasonable approximation for this case, and this is tested in the present experiment.

II. EXPERIMENTAL ARRANGEMENT

The experimental arrangement was that of Dousmanis, Sanders, and Townes,[1] except for the absorption cell which was designed for either Stark or Zeeman modulation. OH was produced by an electrodeless radio-frequency discharge in water vapor, and was then pumped through a glass-lined absorption cell. The glass liner protects radicals from exposure to metal surfaces and also serves as part of the vacuum system, thus eliminating the problem of keeping the waveguide vacuum-tight. Microwave power produced by an X-12 klystron is sent through the absorption cell and is then detected by means of a microwave crystal and a lock-in detector operating at 100 kc/sec, the effective frequency of the Stark or Zeeman modulation.

A typical cross section of the absorption cell is shown in Fig. 1. Teflon spacers are used to support a brass septum in a brass waveguide, about 6 ft long with an outside cross section $1\frac{1}{2}$ in.$\times$2 in. Vacuum-tight cells made of type-7070 glass, which has a relatively small loss tangent at microwave frequencies, are placed above and below the septum. The wall thickness of the glass cells is about 0.050 in., and the sides of the cells are rounded to reduce strains. These cells have gas input and output tubes (not shown) made of 15-mm glass tubing that pass through the top and bottom faces of the waveguide near each end.

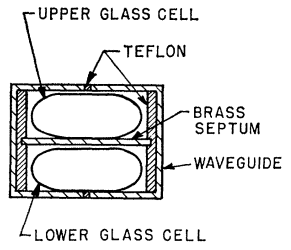

FIG. 1. Cross section of absorption cell.

The brass septum is connected to the inner conductors of four uhf connectors (not shown), which are mounted on the outside of the waveguide. These connectors are on the right- and left-hand sides a few inches from each end of the cell. A radio-frequency voltage can be applied to any one of these connectors in order to obtain Stark modulation.

Initial attempts to observe OH in a different absorption cell with square-wave Stark modulation were unsuccessful, perhaps because the dc component of the applied voltage did not penetrate into the region inside the glass liner. This would be possible if the glass liner had adsorbed water or other polar gas molecules. The interfacial dielectric constant between two materials of different dielectric constant can be extremely large and also can be much greater at dc than at the modulation

* Submitted in partial fulfillment of the requirements for the degree of Doctor of Philosophy, in the Faculty of Pure Science, Columbia University.

† This research was supported in part by the U. S. Army Signal Corps under Contract DA 36-039 SC 78330.

‡ Present address: Laboratory of Biophysics, National Institute of Neurological Diseases and Blindness, National Institutes of Health, Bethesda 14, Maryland.

[1] G. C. Dousmanis, T. M. Sanders, Jr., and C. H. Townes, Phys. Rev. **100**, 1735 (1955).

[2] H. E. Radford, Phys. Rev. **122**, 114 (1961).

frequency used in this experiment (Maxwell-Wagner effect).[3,4]

In the experiments described in this paper, sinusoidal Stark modulation with no dc component was employed. This choice was possible because the transitions of interest in these experiments have quadratic Stark effect. For an applied electric field which is sinusoidal in time, the square of the field has two components: a dc component and a component varying at twice the frequency of the applied field. In order to obtain an effective modulation frequency of 100 kc/sec, it was necessary to use sinusoidal modulation of 50 kc/sec. Therefore, a frequency divider was used to convert the 100-kc/sec signal from the reference oscillator to a 50-kc/sec signal, which was then amplified and applied to the absorption cell.

Instead of the Stark modulation described above, a type of Zeeman modulation similar to the coaxial Zeeman modulation of Ehrenstein, Townes, and Stevenson[5] can be employed. The connectors at the far end of the cell are shorted to the waveguide and a radio-frequency current is sent through a connector on the near side. In this way current will flow down the septum and back along the waveguide, thus producing a magnetic field which is largely confined to the region inside or near the waveguide. This provides Zeeman modulation of the absorption cell with relatively little pickup in the detecting circuits.

The waveguide has been cut in half and then held together with Teflon spacers between the halves and bakelite supports (not shown) along the outside of the waveguide. This was done for two reasons: first, to facilitate assembly, and second, to allow a slightly different method of Zeeman modulation from that described above, one that will provide approximately twice the modulating field for a given current provided by an external modulator. This method of Zeeman modulation is as follows:

Two brass septa, insulated from each other, are substituted for the one indicated in Fig. 1, each approximately one-half the width of the original. This substitution provides two inner current paths. Because the waveguide halves are insulated from each other, there are two outer current paths. These four elements are placed in series by means of the uhf connectors in such a way that current flows down the right inner conductor, back along the right outer conductor, down the left inner conductor and back along the left outer conductor. In this method, the resistance along the path of the modulating current is increased, but since this resistance is small compared to the resistance of the external modulator, this effect is unimportant.

In order to provide adequate Zeeman modulation, current amplitudes of about 25 A are required, even with the double septum. These currents were obtained by making the absorption cell part of a tuned circuit with a resonant frequency of 100 kc/sec and a Q of about 40. A toroidal coil of copper tubing was used for the inductor of the tuned circuit in order to minimize stray fields. In addition, the entire tuned circuit, except for the waveguide and coaxial cable leading to it, was enclosed in a copper box. A continuous water flow was maintained through the copper tubing to prevent overheating. Because the circuit was tuned, square-wave modulation could not be employed. For the transitions of interest in these experiments, the Zeeman effect is linear, and so unbiased sinusoidal current would not provide any modulation. Therefore, a direct current, obtained from storage batteries, was superimposed on the 100-kc/sec sinusoidal current.

III. $O^{17}H$ HYPERFINE STRUCTURE

The energy level diagram for the $J=7/2$ state of $O^{17}H$ is shown in Fig. 2, which is not to scale. In the absence of hyperfine structure, the state would be split by an amount ν_0 into two Λ-doubling levels, because of interaction between the molecular rotation and the electronic motion. Because of the O^{17} nuclear spin of $\frac{5}{2}$, hereafter referred to as I_1, each Λ-doubling level is split into six F_1 levels. Because of the H nuclear spin of $\frac{1}{2}$, hereafter referred to as I_2, each F_1 level is split further into two F levels. With this level structure there are 42 allowed transitions between the upper and lower Λ-doubling levels. In general, the strongest lines correspond to transitions with $\Delta F=0$, $\Delta F_1=0$. These are called main lines, and all other transitions are called satellites.

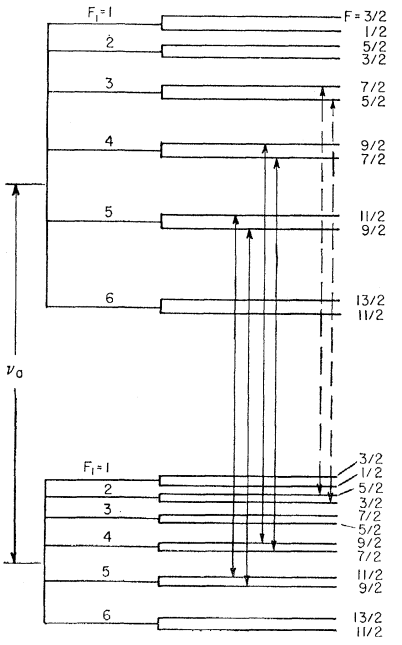

FIG. 2. Energy level diagram for $J=7/2$ level of $O^{17}H$.

[3] C. Kittel, *Introduction to Solid State Physics* (John Wiley & Sons, Inc., New York, 1956), p. 175.
[4] K. W. Wagner, Arch. Elecktrotech. 2, 371 (1914).
[5] G. Ehrenstein, C. H. Townes, and M. J. Stevenson, Phys. Rev. Letters 3, 40 (1959).

For OH Λ-doubling lines, sinusoidal Zeeman modulation provides greater accuracy in frequency determination than does sinusoidal Stark modulation because the latter displaces the center of a line whereas the former broadens a line symmetrically. This can be explained as follows:

During the half-cycle of effective modulation corresponding to "field off," there is a small but nonzero effective field for either sinusoidal Stark or sinusoidal Zeeman modulation. Because the Stark effect arises as a second-order perturbation, the frequency separation between the two members of the Λ doublet always increases in the presence of an effective electric field. Thus, when sinusoidal Stark modulation is employed, a Λ-doubling line is always displaced towards higher frequency. With Zeeman modulation, on the other hand, the components of each member of the Λ doublet corresponding to different values of the quantum number M are displaced up or down in energy according as M is positive or negative. Furthermore, the selection rule is $\Delta M = \pm 1$. Components of a Λ-doubling line with $\Delta M = +1$ and components with $\Delta M = -1$ are displaced in opposite directions. Thus, when sinusoidal Zeeman modulation is employed, a Λ-doubling line is broadened, but its center frequency is not displaced.

The spectrum of $O^{17}H$ obtained from a discharge in ordinary water has very weak lines both because of the large number of lines present and because of the small natural abundance of O^{17}. In order to obtain sufficient intensity to observe $O^{17}H$ spectral lines, we used water enriched to 3.3 at. % of O^{17} in the discharge. Because only a limited quantity of enriched water was available, special emphasis was placed on equipment reliability. Both Stark and Zeeman modulations were used in preliminary tests with $O^{16}H$, and were found to give equal line intensities, but Zeeman modulation was found to be less reliable over long periods because of the requirement for storage batteries and cooling water. Accordingly, sine wave Stark modulation was used for the $O^{17}H$ spectra, despite the resultant frequency displacement.

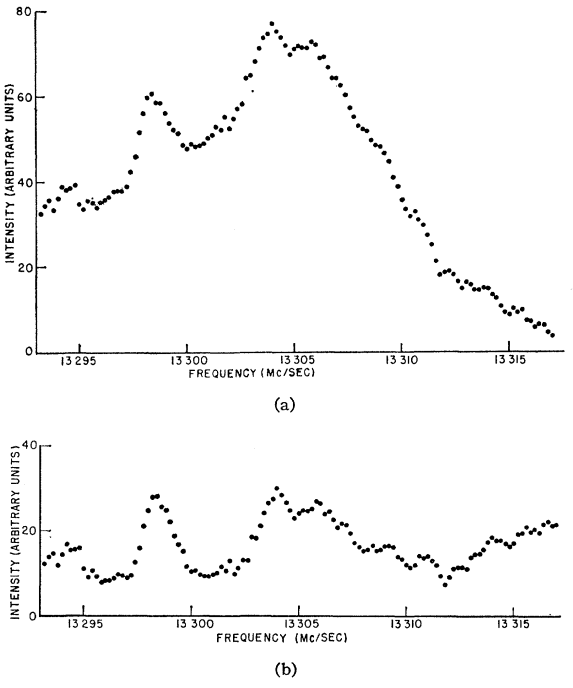

FIG. 3. (a) Portion of $O^{17}H$ spectrum including $F_1=5 \leftarrow F_1=5$ transitions (uncorrected). (b) Portion of $O^{17}H$ spectrum including $F_1=5 \leftarrow F_1=5$ transitions (corrected).

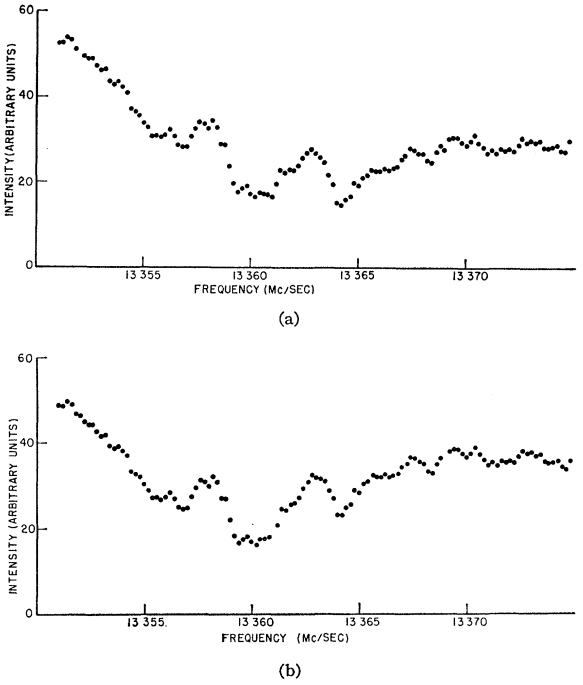

FIG. 4. (a) Portion of $O^{17}H$ spectrum including $F_1=4 \leftarrow F_1=4$ transitions (uncorrected). (b) Portion of $O^{17}H$ spectrum including $F_1=4 \leftarrow F_1=4$ transitions (corrected).

The corrections to be applied because of this frequency displacement were determined from the theoretical Stark pattern for each transition and the known displacement for $O^{16}H$. These corrections are about 0.2 Mc/sec and are accurate to about ±0.02 Mc/sec. The additional error thus introduced is not important for the $O^{17}H$ measurements, because the low signal-to-noise ratio resulted in experimental uncertainties of about ±0.3 Mc/sec. If the system we have described were to be used for frequency measurements of accuracy comparable to ±0.02 Mc/sec, then Zeeman modulation should be employed.

Four main lines (two doublets) of the $O^{17}H$ hyperfine structure for the $^2\pi_{3/2}$, $J=7/2$ Λ-doubling transition have been observed. For each doublet, four experimental runs were taken over the desired frequency region with O^{17}-enriched water in the discharge, and the results were averaged. These averaged $O^{17}H$ spectra are shown in Figs. 3(a) and 4(a). Also, comparison runs

TABLE I. Experimentally measured main lines in $O^{17}H$ hyperfine structure for the $^2\pi_{3/2}$ $J=7/2$ state.

	$F_1=5 \leftarrow F_1=5$	$F_1=4 \leftarrow F_1=4$
Lower frequency (Mc/sec)	13 298.20±0.2	13 358.06±0.3
Higher frequency (Mc/sec)	13 304.08±0.3	13 363.06±0.3
Experimental hyperfine doublet separation (Mc/sec)	5.88±0.4	5.00±0.4
Hyperfine doublet separation determined from $O^{16}H$ data (Mc/sec)	5.52±0.15	4.97±0.13
Frequency in absence of I_2 (Mc/sec)	13 301.41±0.2	13 360.84±0.2

were made over the same frequency regions with ordinary water, in order to determine any frequency-dependent variations in the output of the system due to causes other than the $O^{17}H$ spectrum. The results for the comparison runs were subtracted from the averaged $O^{17}H$ results, and these corrected, averaged $O^{17}H$ spectra are shown in Figs. 3(b) and 4(b). The measured frequencies for the main lines are listed in Table I.

In order to determine hyperfine constants about O^{17}, it was necessary to assign F_1 values to the observed lines. For each possible assignment of F_1 values to the four main lines, ν_0 was determined from the experimentally determined frequencies of the main lines and the interval rule. Only one assignment of F_1 values gives satisfactory agreement with the value of ν_0 calculated from the theory of Dousmanis, Sanders, and Townes.[1] Based on this assignment, the observed lines are indicated by solid arrows in Fig. 2. A measure of the accuracy of this theory can be obtained by comparing theoretical values of ν_0 in $O^{16}H$ and $O^{18}H$ with values of ν_0 determined from the experimentally measured frequencies of the main lines. For $O^{16}H$ and $O^{18}H$, there is no problem of quantum number assignments because there are only two main lines in each spectrum. Accordingly, the spectrometer described above was used to determine the experimental value of ν_0 for $O^{18}H$. The value for $O^{16}H$ has been reported previously.[1] Experimental values of ν_0 for $O^{16}H$ and $O^{18}H$ and for $O^{17}H$ with the F_1 assignments shown in Fig. 2 are compared with values calculated from theory in Table II.

It can be seen from Table II that with these F_1 assignments the experimental value of ν_0 for $O^{17}H$ agrees with the theory to the accuracy of the latter. For all other F_1 assignments, experimental and calculated values of ν_0 for $O^{17}H$ differ from each other by at least 60 Mc/sec.

The hyperfine doublet splittings for $O^{17}H$ depend upon the hyperfine constants about the proton, and not upon the hyperfine constants about O^{17}. Hence, the hyperfine doublet splittings for $O^{17}H$ can be obtained from previous work on $O^{16}H$ hyperfine structure.[1] These values are compared with experimental hyperfine doublet splittings for $O^{17}H$ in Table I. Agreement is within experimental error, providing an additional check on the F_1 assignments.

Although the presence of I_2 and the corresponding hyperfine doublet splittings are useful in the identification of lines, analysis of hyperfine constants about O^{17} can best be made after elimination of the effect of I_2. Since the hyperfine doublet splittings are due to interactions of the form $I_2 \cdot F_1$, the frequency of each F_1 transition in the absence of nuclear spin I_2 can be easily computed from the experimental data. These frequencies are listed in Table I, and their separation, hereafter referred to as Δ, is 59.43 Mc/sec.

In the absence of I_2, the theoretical hyperfine energy for the upper Λ-doubling level is of the form $(Z+Y)I_1 \cdot J$, and for the lower Λ-doubling level, $(Z-Y)I_1 \cdot J$.[1] Z and Y depend upon accurately known molecular properties of OH and upon the hyperfine coupling constants for diatomic molecules defined by Frosch and Foley[6] and by Dousmanis[7]:

$$a=2\mu_0\frac{\mu_{I_1}}{I_1}(1/r^3)_{\mathrm{av}},$$

$$b=-\mu_0\frac{\mu_{I_1}}{I_1}\left[\frac{(3\cos^2\chi-1)}{r^3}\right]_{\mathrm{av}}+\frac{16\pi}{3}\mu_0\frac{\mu_{I_1}}{I_1}\psi^2(0),$$

$$c=3\mu_0\frac{\mu_{I_1}}{I_1}\left[\frac{(3\cos^2\chi-1)}{r^3}\right]_{\mathrm{av}}$$

$$d=3\mu_0\frac{\mu_{I_1}}{I_1}\left[\frac{\sin^2\chi}{r^3}\right]_{\mathrm{av}}.$$

μ_0 is the Bohr magneton (taken as positive), and μ_{I_1} and I_1 are the nuclear magnetic moment and spin, respectively, of O^{17}. r is the distance from the O^{17} nucleus to the unpaired electron, and χ is the angle at the O^{17} nucleus between the unpaired electron and the internuclear axis. $\psi^2(0)$ is the probability density of electron spin at the O^{17} nucleus. Y is proportional to the hyperfine constant d, and Z is a linear combination of hyperfine constants a, b, and c;

$$Y=d\left[\frac{\left(x-2+\frac{A}{B}\right)(J+\frac{1}{2})}{4xJ(J+1)}\right]$$

$$Z=\frac{1}{4xJ(J+1)}\left\{2a\left[2x+2-\frac{A}{B}\right]\right.$$

$$\left.+b\left[4(J-\tfrac{1}{2})(J+\tfrac{3}{2})+x+4-2\frac{A}{B}\right]+c\left[x-4-2\frac{A}{B}\right]\right\}.$$

A and B are the fine structure constant and the rotational constant, respectively, and

$$X\equiv\left[4(J+\tfrac{1}{2})^2+\frac{A}{B}\left(\frac{A}{B}-4\right)\right]^{1/2}.$$

[6] R. A. Frosch and H. M. Foley, Phys. Rev. 88, 1347 (1952.)
[7] G. C. Dousmanis, Phys. Rev. 97, 967 (1955).

TABLE II. OH Λ-doubling frequencies for the $^2\pi_{3/2}$ $J=7/2$ state.

Isotopic species	ν_0 exp (Mc/sec)	ν_0 calc (Mc/sec)	ν_0 exp $-\nu_0$ calc (Mc/sec)
$O^{16}H$	13 438.41±0.05[a]	13 430.4	8.0
$O^{17}H$	13 334.09±0.3	13 319.9	14.2
$O^{18}H$	13 234.16±0.1	13 222.5	11.7

[a] Measured by Dousmanis, Sanders, and Townes (reference 1).

For main lines, $I_1 \cdot J$ is the same for the upper and lower Λ-doubling levels, and so the corresponding hyperfine energies are proportional to the parameter Y, but do not depend upon Z. The frequency separation between main lines, of course, is also proportional to Y, and hence is proportional to the hyperfine constant d. In particular, the frequency separation between the observed main lines, Δ, is proportional to d. After the appropriate molecular constants are evaluated, there results:

$$\Delta = 0.1431d.$$

The constant of proportionality is accurate to four significant figures. From the experimentally determined value of Δ,

$$d = -415.3 \pm 2.0 \text{ Mc/sec}.$$

The constant d can also be determined theoretically from its definition by the use of a simple model. The electronic structure may be taken as[8] $(1s\sigma)^2(2s\sigma)^2(2p\sigma)^2(2p\pi)^3$, with one unpaired $p\pi$ electron about the O^{17} nucleus. Then $(\sin^2\chi)_{av}=0.8$. To determine $(1/r^3)_{av}$ for OH, the value determined from the fine structure of the ground state of the oxygen atom[9] must be corrected to allow for the partial ionic character of OH. For the negatively ionized oxygen atom, the electrons will be more loosely bound than for the neutral atom; r will increase and $(1/r^3)$ will decrease. The ionic correction was computed, using empirical approximations of Dailey and Townes.[10] It was found that the ionic character decreases $(1/r^3)_{av}$ by about 11–15%. The best value for $(1/r^3)_{av}$ is 29.9×10^{24} cm^{-3}. The remaining constants in the definition of d are accurately known. The value of d calculated under the assumptions indicated above is

$$d = 384 \text{ Mc/sec}.$$

This is in good agreement with the value of d determined experimentally, but the experimental value is greater in magnitude by 7.6%. As much as one-third of this difference may be due to the approximate nature of the ionic correction. Nevertheless, it is reasonably certain that the experimental value of d is greater in magnitude than that determined from the simple model. Similar results have been reported for the NO molecule[7] and for the $O^{16}O^{17}$ molecule.[11] The experimental results for NO indicate that the probability for the unpaired electron to be on the N atom is 0.65. The experimental value of $(\sin^2\chi/r^3)_{av}$ about the N nucleus is 8% greater in magnitude than the theoretical value based on a pure atomic $p\pi$ wave function and the above probability. For $O^{16}O^{17}$, the experimental value of $(3\cos^2\chi-1/2r^3)_{av}$ about O^{17} was found to be 15% greater in magnitude than the theoretical value based on one electron with a pure atomic $p\pi$ wave function about O^{17}. This corresponds to an experimental value of $(\sin^2\chi/r^3)_{av}$ about 3% greater than the theoretical value for a $p\pi$ wave function. The results for NO, O_2, and OH taken together suggest that an apparent atomic $p\pi$ wave function in a diatomic molecule is somewhat compressed in a plane perpendicular to the internuclear axis.

Figures 3(a) and 3(b) show two small bumps in addition to the two members of the $F_1=5$ hyperfine doublet. One of these is near 13 294 Mc/sec and the other near 13 306 Mc/sec. These bumps are not much larger than the noise level, and cannot be definitely identified as spectral lines. If either were a spectral line, it would have to be a satellite, and this would require another satellite line of about equal intensity about 4.6 Mc/sec away. This requirement tends to eliminate the higher frequency bump as a possible satellite. Furthermore, comparison of Fig. 3(a) and 3(b) shows that the frequency of the higher frequency bump corresponds to the extremum of the background. Thus, it seems quite likely that the higher frequency bump is due to imperfect cancellation of frequency-dependent background.

The lower frequency bump is not eliminated by the requirement of the existence of another satellite 4.6 Mc/sec away, because there is a main line about 4.6 Mc/sec away on one side, and the data do not extend sufficiently far on the other side. Furthermore, the lower frequency bump looks like a spectral line on both Figs. 3(a) and 3(b), and the apparent intensity of that line (approximately one-fourth of the main line) corresponds to the theoretical intensity of the possible satellite lines to be considered. Therefore, we have tentatively assumed that the lower frequency bump is a satellite. The following analysis is based on this assumption.

The frequency of a satellite depends upon both Y and Z. Since Y is known from analysis of the main lines, Z can be determined experimentally from the position of the satellite line if the transition can be properly identified. If the satellite transition is $F_1=3 \leftarrow F_1=2$, $F=7/2 \leftarrow F=5/2$, then $Z=-44.5$ Mc/sec. If the satellite transition is $F_1=3 \leftarrow F_1=2, F=5/2 \leftarrow F=3/2$, then $Z=-43.1$ Mc/sec. These two possibilities are indicated by dashed arrows in Fig. 2. For all other transitions, Z values computed from the experimental satellite frequency differ from the theoretical Z value computed below by at least a factor of 2.

Z is a linear combination of a, b, and c, and can be computed theoretically from their definitions and a

[8] R. S. Mulliken and A. Christy, Phys. Rev. **38**, 87 (1931).
[9] T. Yamanouchie and H. Horie, J. Phys. Soc. Japan **7**, 52 (1952).
[10] B. P. Dailey and C. H. Townes, J. Chem. Phys. **23**, 118 (1955).
[11] S. L. Miller, C. H. Townes, and M. Kotani, Phys. Rev. **90**, 542 (1953).

model similar to the simple model used above to obtain a value for d in good agreement with experiment. The result of this computation for Z is

$$Z=-28.0-(10.6\times10^{-24})\psi^2(0)\ \text{Mc/sec}.$$

According to the simple model, $\psi^2(0)$ should be zero, since the electron under consideration has a $p\pi$ wave function. However, experimental results for the NO molecule[7] and the O^2 molecule[11] indicate that, in cases similar to that of the OH radical, an electron expected to have a $p\pi$ wave function actually has about 2.5% s character. If it is assumed that the unpaired electron in OH also has 2.5% s character, then $\psi^2(0)=1.26\times10^{24}$ cm^{-3}, and $Z=-41.4$ Mc/sec. This differs from the experimental value of Z, as determined for either of the satellite transitions indicated in Fig. 2, by less than 8%.

IV. DIPOLE MOMENT MEASUREMENT

The $^2\pi_{3/2}$, $J=7/2$, $M=4$ Λ-doubling line of $O^{16}H$ was selected for Stark shift measurements because of its relatively high intensity and relatively large Stark shift. For quadratic Stark effect,

$$\Delta f=K\mu^2E^2, \tag{1}$$

where Δf=change in center frequency of line (Stark shift), μ=dipole moment, and E=electric field. For the OH transition of interest, K can be expressed in terms of the Stark coefficients for the case of no hyperfine structure,[12] which, in turn, can be simply determined from perturbation theory.

Since the two members of the Λ doublet are very close together compared to all other levels, and since the Stark shift is very much smaller than the Λ-doubling frequency, the Stark shift for the case of no hyperfine structure is:

$$(\Delta f)_0=2\mu^2E^2\cos^2\alpha\cos^2\beta/\nu_0, \tag{2}$$

where μ=electric dipole moment, ν_0=Λ-doubling frequency, α=angle between internuclear axis and **J**, and β=angle between **J** and **E**. Since ν_0, $\cos\alpha$, and $\cos\beta$ are calculable from known molecular parameters for OH and the vector model, Eq. (2) can be used to determine the Stark coefficients for the case of no hyperfine structure.

$$\text{Cos}^2\alpha=\frac{1}{4x^2J(J+1)}\left\{\frac{1}{4}\left[x-2+\frac{A}{B}\right]^2+\frac{9}{4}\left[x+2-\frac{A}{B}\right]^2+\frac{3}{2}\left[x^2-\left(2-\frac{A}{B}\right)^2\right]\right\},$$

$$\cos^2\beta=\frac{M_J^2}{J(J+1)}.$$

[12] C. H. Townes and A. L. Schawlow, *Microwave Spectroscopy* (McGraw-Hill Book Company, Inc., New York, 1955), p. 260.

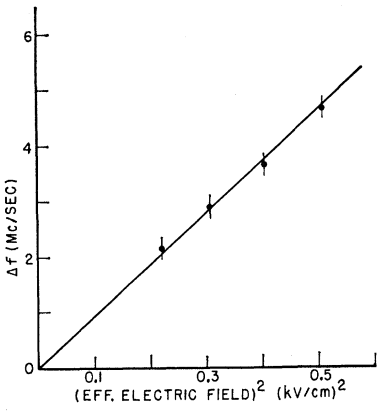

FIG. 5. Stark shift vs (effective electric field) (reference 2).

For the OH transition of interest, $K=3.61$(Mc/sec)/$[\text{D}^2\ (\text{kV})^2\ \text{cm}^{-2}]$ so that

$$\Delta f=3.61\mu^2E^2.$$

In order to find μ, Δf was determined for several values of electric field between 0.47 and 0.71 kV/cm. This was done by using Stark modulation and measuring the frequencies of the Stark components.

We were not able to resolve the individual OH Stark components corresponding to different M values. Instead, for each experimental spectrum we determined the center of the unresolved composite line, and then applied a correction to obtain the center of the $M=4$ line. Since the intensities and shifts of the Stark components are proportional to M^2, the correction is a small percentage of the Stark shift for the $M=4$ line. In order to obtain the correction, the theoretical position of the center of a composite line—the sum of Lorentzian lines corresponding to each of the Stark components—was determined as a function of the Stark shift of the $M=4$ line with the help of a computer. The corrections were about 3% of the Stark shifts.

A radio-frequency voltmeter was used to measure the voltage between the septum and the outside of the waveguide. The "effective" electric field was determined as a function of this voltage by measuring Stark shifts of a molecule of known dipole moment. The calibration was made by an observation of the $2_2\leftarrow2_1$ rotational transition of HDO; the value of $K\mu^2$ for this transition has been experimentally determined,[13] and the effective value of E^2 is found from Eq. (1). With this method of calibration, it is only necessary that the voltmeter be linear.

Figure 5 is a plot of corrected Stark shift vs square of effective electric field. According to Eq. (3), the slope of the best straight line through the points equals $3.61\mu^2$. The value of the dipole moment obtained from the measured slope is 1.60 ± 0.12 D. The experimental error quoted is primarily due to the scatter of points in Fig. 5.

We have previously reported a preliminary value for the OH dipole moment of 2.1 ± 0.4 D,[14] in marginal

[13] M. W. P. Strandberg, J. Chem. Phys. **17**, 901 (1949).
[14] G. Ehrenstein, Bull. Am. Phys. Soc. **6**, 20 (1961).

agreement with the present value. The preliminary value was obtained before the rectangular glass cells were fabricated, and was based on spectra obtained with a single glass cell of circular cross section. The circular cell has a filling factor of about $\frac{1}{8}$ and a correspondingly small signal-to-noise ratio.

The present value is in good agreement with the value of 1.54 D obtained by Madden and Benedict[15] from the infrared emission spectrum of an oxy-acetylene flame and estimates of the $OH:H_2O$ concentration ratio. Although the concentration ratio estimates now seem to have been quite accurate, this was not known at the time they were made, and Madden and Benedict were not able to assign an experimental error to their value of dipole moment.

The present value is also in good agreement with the value of 1.65 ± 0.25 D recently obtained by Meyer and Myers, using microwave spectroscopy.[16] They used square-wave Zeeman modulation to facilitate detection and observed the Stark shift due to the application of a dc electric field between two parallel aluminum plates. Their observations were made on the $^2\pi_{3/2}$, $J=9/2$ Λ-doubling lines. The experimental error they quote is somewhat greater than ours, probably due to the fact that their maximum observed Stark shifts were about 1.2 Mc/sec—somewhat smaller than ours (see Fig. 5).

Meyer and Myers also point out that their experimental results indicate that the OH dipole moment is close to the OH bond moment found in water, 1.53 D, but outside the range of the most complete theoretical calculations, which give values between 2.1 and 2.7 D. This is confirmed by the present results.

[15] R. P. Madden and W. S. Benedict, J. Chem. Phys. **23**, 408 (1955).

[16] Richard T. Meyer and Rollie J. Myers, J. Chem. Phys. **34**, 1074L (1961).

V. CONCLUSIONS

The electric dipole moment for OH has been found to be 1.60 ± 0.12 D.

Four main lines (two doublets) of the $O^{17}H$ hyperfine structure for the $^2\pi_{3/2}$, $J=7/2$ Λ-doubling transition have been observed. The doublet splittings are in agreement with doublet splittings computed from hyperfine structure constants obtained from experiments on $O^{16}H$. The separation between the doublets gives a value of $d=-415.3\pm2.0$ Mc/sec, in good agreement with a simple model that assumes one unpaired $p\pi$ electron about the O^{17} nucleus.

ACKNOWLEDGMENTS

I would like to thank Professor C. H. Townes for his valuable advice and encouragement, Harold Lecar for his help in carrying out the $O^{17}H$ experimental runs, the IBM Watson Laboratory for the use of a 650 computer, and the entire staff of the Columbia Radiation Laboratory for a wide range of helpful services.

PHYSICAL REVIEW VOLUME 130, NUMBER 2 15 APRIL 1963

Theory of Cavity Masers

D. E. McCumber

Bell Telephone Laboratories, Murray Hill, New Jersey

(Received 6 August 1962; revised manuscript received 16 January 1963)

Simple interference experiments identify correlation functions which describe the response of maser amplifiers and the output of maser oscillators. General operator techniques are used to evaluate these functions in cavity maser systems for which the coupling of the maser electromagnetic field to external energy sources or sinks is mediated by systems whose short-term response depends primarily upon average or macroscopic system properties. The dielectric theory which results includes only those short-term nonlinearities associated with the external pumping fields. In the long term both the external and the cavity fields can modify the susceptibility functions. The techniques utilized permit a detailed analysis of approximations and suggest generalizations for increased precision. As one important result of this type the theory indicates that macroscopic rate equations are valid if modulation frequencies are much less than the width of the narrowest coupling system spectral line.

I. INTRODUCTION

As refined experimental procedures continue to probe more deeply the mechanisms underlying maser action[1] in spectral regions ranging from microwave to optical frequencies, it has become increasingly more important to scrutinize the simple approximations which underlie the existing mathematical analyses[2] and to develop generalizations which are valid for broad classes of maser systems. In this context the present paper has three basic objectives: to determine un-

[1] J. P. Gordon, H. J. Zeiger, and C. H. Townes, Phys. Rev. **95**, 282 (1954); **99**, 1264 (1955).

[2] A survey of a number of approaches with an extensive annotated bibliography has been given by W. E. Lamb, Jr., in *Lectures in Theoretical Physics, III, University of Colorado Summer School 1959*, edited by W. E. Britten, B. W. Downs, and J. Downs (Interscience Publishers, Inc., New York, 1960), p. 435.